

# Cerenkov luminescence imaging and applications

Subjects: Nanoscience & Nanotechnology

Contributor: Antonello Spinelli

Cerenkov luminescence imaging (CLI) is a novel optical molecular imaging modality based on the detection of the Cerenkov radiation.

Keywords: nanoparticles ; nanocompounds ; nanoclusters ; cerenkov radiation ; cerenkov luminescence imaging ; photodynamic therapy ; gold nanoparticles ; silica nanoparticles ; rare-earth nanoparticles

---

## Overview

Cerenkov luminescence imaging and Cerenkov photodynamic therapy have been developed in recent years to exploit the Cerenkov radiation (CR) generated by radioisotopes, frequently used in Nuclear Medicine, to diagnose and fight cancer lesions. For in vivo detection, the endpoint energy of the radioisotope and, thus, the total number of the emitted Cerenkov photons, represents a very important variable and explains why, for example,  $^{68}\text{Ga}$  is better than  $^{18}\text{F}$ . However, it was also found that the scintillation process is an important mechanism for light production. Nanotechnology represents an important field, providing nanostructures which are able to shift the UV-blue emission into a more suitable wavelength, with reduced absorption, which is useful especially for in vivo imaging and therapy applications. Nanoparticles can be made, loaded or linked to fluorescent dyes to modify the optical properties of CR radiation. They also represent a useful platform for therapeutic agents, such as photosensitizer drugs for the production of reactive oxygen species (ROS). Generally, NPs can be spaced by CR sources; however, for in vivo imaging applications, NPs bound to or incorporating radioisotopes are the most interesting nanocomplexes thanks to their high degree of mutual colocalization and the reduced problem of false uptake detection. Moreover, the distance between the NPs and CR source is crucial for energy conversion. Here,

## 1. Introduction

Cerenkov luminescence imaging (CLI) was introduced a decade ago and is becoming an established imaging modality. Nowadays, applications include preclinical molecular imaging, surgery, external beam radiotherapy, photodynamic therapy and endoscopy. Several reviews focusing on CLI discovery and applications can be found in literature [\[1\]](#)[\[2\]](#)[\[3\]](#)[\[4\]](#)[\[5\]](#).

As will be described in more detail, the main problems with CLI are the low light yield and a radiation spectrum shifted towards the ultraviolet (UV)-blue region. These can become limiting factors for in vivo imaging, considering the high tissue absorption in this wavelength range [\[6\]](#). In order to overcome the intrinsic limitations related to the emission of Cerenkov radiation (CR), different approaches based on the use of nanoparticles (NP) have been developed.



**Figure 1.** Schematic representation of the Cerenkov light emission process. A beta particle, emitted by a radionuclide, travels in a medium faster than the light speed in the medium itself. The fast de-polarization of the molecules produces a cone of light known as Cerenkov radiation.

## 2. Nanoparticles for Imaging and Therapy Using Cerenkov Sources

### 2.1. Nanoparticles

A plethora of NPs or nanocompounds were tested to evaluate their interaction with CR sources, both for imaging and therapeutic purposes. The first attempts were made using quantum dots (QDs), because they are very bright and stable [7]. QDs are composed of a CdSe 1–6 nm-sized core, sometimes containing Te to shift the emission toward the 750–800 nm wavelength, which is useful for in vivo applications. Outside the core, their structure presents an inner shell of ZnS and an outer shell often composed of polyethylene glycol (PEG) to improve biocompatibility (Figure 2a).

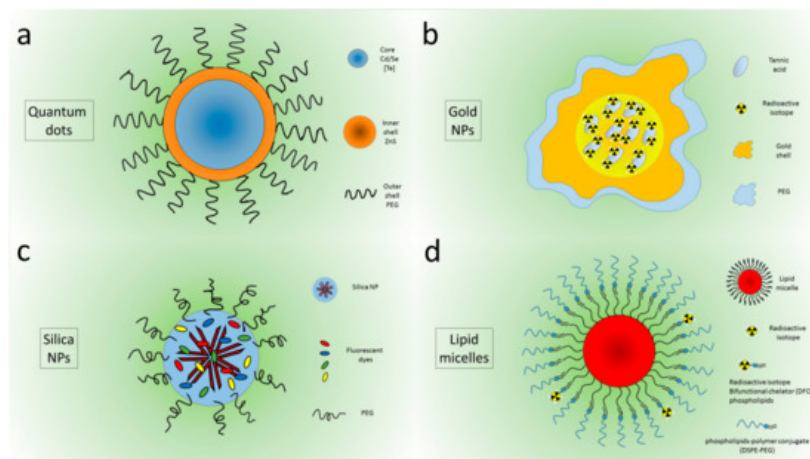


**Figure 2.** Pegylated Quantum dots (a), Au nanoparticles (b) Silica Nanoparticles (c), micelles (d).

They have an efficiency which is 20–30 times higher than that of organic fluorophores, size-tunable emission, an extremely broad excitation range and narrow emission which allow large Stokes shifts to occur [8]. In pioneering works, QDs were initially used as free NPs separated from the CR source [9][10][11][12]. They were then doped with  $^{64}\text{Cu}$  by Sun et al. [13] to synthesize self-illuminating NPs exhibiting high Cerenkov resonance energy transfer (CRET). QDs showed no dissociation of  $^{64}\text{Cu}$  from the NPs, and their application in in vivo tumor imaging made it possible to obtain a PET confirmation. In 2017, Zhao et al. used QDs encapsulated with  $^{89}\text{Zr}$  in lipid micelles to obtain a bimodal tracer to study pharmacokinetics and biodistribution in whole body imaging via PET and CLI [14]. Unfortunately, QDs contain toxic elements like cadmium, and thus, require external passivation for in vivo imaging applications, raising concerns about their synthesis procedures. Alternative materials with fewer safety and environmental risks are, therefore, of interest for this kind of application. For this purpose, many different NPs have been tested in the literature. Gold nanoparticles, rare earth nanophosphors, lipid nanomicelles, silica nanoparticles and titanium dioxide NPs are the most investigated compounds.

Au nanocages incorporating  $^{189}\text{Au}$  atoms were first proposed by Wang et al. in 2013, showing emission in the visible and near-infrared range and allowing the imaging of whole animals in vivo [15]. In 2014, self-illuminating gold nanoclusters doped with  $^{64}\text{Cu}$  were designed for bimodal imaging (PET and CLI) [16]. In the same year, nanostructures with a similar size but four different shapes (nanospheres, nanodisks, nanorods, and cubic nanocages) incorporating radioactive  $^{198}\text{Au}$  were investigated. The PEGylated Au nanostructures were injected intravenously in tumor-bearing mouse, and CLI was used to detect the biodistribution in vivo, confirming the results obtained with autoradiographic imaging on slices of the tumor after excision. In particular, the results showed a higher tumor uptake for the nanospheres and nanodisks compared to the nanorods and nanocages at 24 h postinjection. Interestingly, nanospheres and nanodisks were observed only on the boundaries of the cancer masses, while nanorods and nanocages were distributed throughout the tumors [17]. Gold nanoclusters conjugated with blood serum proteins were used to convert beta-decaying radioisotope energy into tissue-penetrating optical signals with both  $^{18}\text{F}$  and  $^{90}\text{Y}$  [18]. Lee et al. showed that PEGylated radioiodine-embedded gold nanostructures (Figure 2b) are promising potential lymphatic tracers in biomedical imaging for pre- and intra- operative surgical guidance [19][20].

Hollow mesoporous silica NPs and nanoshells were applied principally in photodynamic therapy (PDT); doped with  $^{89}\text{Zr}$ , they were used to activate chlorin e6 (C6) and porphyrin to produce reactive oxygen species (ROS) to damage cancer cells [21][22]. Amorphous silica NPs were tested by Pratt et al. [23] in a complete study of both NPs and CR sources. Recently, silica NPs were synthesized containing five different dyes that were chosen to efficiently absorb CR in a wide wavelength range and to efficiently tunnel the excitation energy toward the lowest energy Cy7 derivative dye presenting a fluorescence emission in the near-infrared region (NIR), [24] (Figure 2c).

Lipid calcium phosphate nanoparticles bound with  $^{177}\text{Lu}$  were investigated by Satterlee et al. [25] to perform both anticancer therapy and in vivo imaging, exploiting CLI and SPECT and imaging modalities. Other liposomes containing  $^{188}\text{Re}$  were developed by Chang et al. [26] to reduce proliferation of human and neck cancer cells in vivo. Lipid micelles doped with  $^{89}\text{Zr}$  and containing QDs were investigated by Zhao et al. [14] to image pharmacokinetics and biodistribution using both PET and CLI techniques (Figure 2d).

$\text{TiO}_2$  NPs were investigated almost exclusively for PDT, as shown in the next section. The use of rare earth nanophosphors was suggested in 2011 by Sun et al. [27]. Carpenter et al. [28] demonstrated the down-conversion of Cerenkov light emitted from  $^{18}\text{F}$  by barium yttrium fluoride nanocrystals doped with terbium and europium. Instead, excitation by  $^{68}\text{Ga}$  terbium-doped Gd nanoparticles revealed a significant improvement in detection sensitivity for clinical diagnoses of gastrointestinal tract tumors [29]. The fact that gamma radiation is the major cause of Europium Oxide (EO) NP emissions was demonstrated by Hu et al. [30]. The same group successfully employed EO NPs in cancer detection, even with ultrasmall tumors (less than 1 mm) [31][32].

A great variety of NPs (silica,  $\text{TiO}_2$ , rare earth, gold NPs) were tested by Pratt et al., who investigated both sources and NPs in order to clarify the excitation mechanisms [23] underlying the NP light emission.

Recently, persistent luminescence nanoparticles (PLNPs) with rechargeable near infrared afterglow properties, specifically,  $\text{Cr}^{3+}$ -doped zinc gallate (ZGCs), were proposed in combination with  $^{18}\text{F}$  for tumor diagnosis in living animals, since they can avoid tissue autofluorescence and improve the signal-to-background ratio [33].

## 2.2. Toxicity

In order to evaluate the effects of NPs on living organisms, their toxicity has been investigated in many different modalities. It is worth noting that for diagnostic purposes, safe NPs are requested, as opposed to therapeutic applications, whereby specific cytotoxicity against cancer cells (combined with a high degree of specific uptake) could represent an advantage. In particular, for PDT, NPs need to exhibit low cytotoxicity in the dark and high killing when activated by light. Black et al. [34] evaluated the toxicity of cationic block copolymer NPs in HEK293T cells; the viability was determined by measuring the ATP activity. Lee et al. [19] examined the cytotoxicity of gold NPs on various cell types, including Chinese hamster ovary (CHO) cells, murine macrophage (Raw 264.7) cells, and mouse dendritic (DC2.4 cells) cells using cell viability and apoptosis assays. The results were supported by flow cytometry analysis following annexin V and propidium iodide staining, suggesting that PEG-Rle-AuNPs are not toxic to normal ovarian or immune cells. Besides flow cytometry for in vitro assays, to evaluate the tissue toxicity of EO nanoparticles, Hu et al. [32] examined different organs extracted from human breast (Bcap-37) xenograft mice stained with hematoxylin and eosin (H&E). Goel et al. [22] evaluated the effects of hollow mesoporous silica NPs on white blood cells, red blood cells, mean corpuscular volume, hemoglobin, hematocrit, mean corpuscular hemoglobin, and platelet, collected in mice injected with therapeutic doses of mesoporous silica nanoshells filled with porphyrin at different timepoints after injection. Duan et al. [35] reported the cytotoxicity of the D- $\text{TiO}_2$  NPs evaluated by Cell Counting Kit CCK8 assay. Lee et al. [36] tested PEGylated crushed gold shell-radioactive iodide-124-labeled gold core-124I nanoballs (PEG-Au@AuCBs) with a Cell Counting Kit CCK8 and a CellTiter-Gl Luminescent Cell Viability Assay. Chang et al. [26] used histochemical measurements of stained Ki-67 expression in orthotopic tumors to evaluate the toxicity caused by single and repeated doses of  $^{188}\text{Re}$ -liposomal administrated in tumor-bearing mice.

## 2.3. Radioisotope/Nanoparticle Interaction

Initially, the link between NPs and CR sources was thought of as a simple interaction between Cerenkov photons and fluorescent systems. It subsequently emerged that the beta plus and beta minus particles produced in the decay also interact with the fluorescent systems, releasing the energy needed to emit new photons. For some NPs, gamma emission shows a very low efficiency, and in general, can be ignored [18].

More precisely, radionuclides and NPs can interact in various ways to produce light. NPs can convert the energy released from gamma radiation (gamma scintillation) or beta particle (beta scintillation) into visible photons, or NPs can be excited from photons produced by beta particles (Cerenkov radiation) and deexcited to emit visible photons (with longer

wavelengths) via the so-called Cerenkov radiation energy transfer (CRET). A schematic of the possible interaction is illustrated in [Figure 3](#). In any case, considering the form of energy reaching and emitted by the NPs, interactions can be categorized into two processes: photon–photon and beta–photon emission. For a detailed description of the physical processes behind each kind of interaction, see the work of Pratt et al. [\[23\]](#) and the complete review of Ferreira et al. [\[37\]](#).

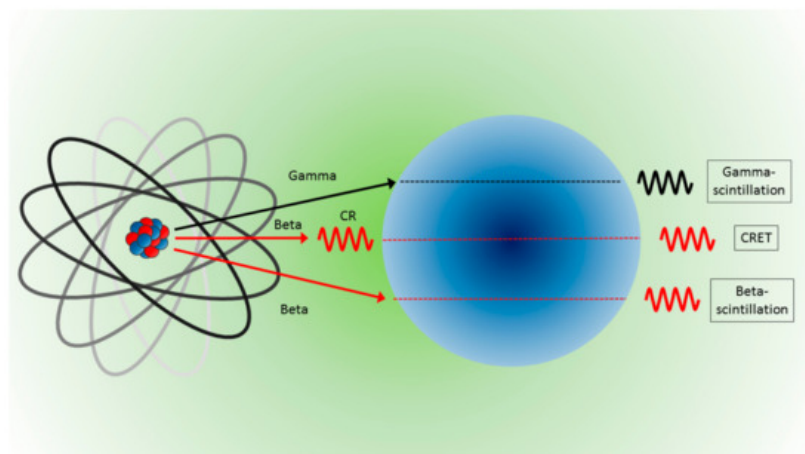


**Figure 3.** Light produced from NPs and the interaction with radionuclides are due to gamma rays which produce gamma scintillation (**top**), interactions with photons (Cerenkov radiation) which are converted by CRET (**middle**), and direct interactions with beta particles which produce beta scintillation (**bottom**).

## 2.4. Optical and Chemical Properties

For imaging purposes, the best NP candidates need to have specific optical properties: absorption spectrum compatible with CR emission, high quantum efficiency and emission in the wavelength range 650–800 nm. This wavelength range of lower optical absorption coefficient is known as tissue transparency window. In cases of excitation via optical photons, the distance between the CR source and the NPs could represent an issue, requiring that NP absorption spectrum be compatible with the red-shifted Cerenkov radiation in the tissue, and that the wavelength of the incoming photons themselves be in the tissue transparency window. In general, the distance, and consequently, the chemical link between the CR source and the NPs is a very important aspect. Nps separated from radionuclides normally have different biodistribution, presenting a low degree of colocalization and reduced CR conversion efficiency.

Separated NPs need to be functionalized in order to reach the same target (generally a tumor mass) as the radionuclide. A simpler strategy is to bind radionuclides and NPs, or encapsulate them therein, or substitute the chemical components of the NPs with radioactive isotopes. Following the review of Shaffer et al. [\[5\]](#), NPs were subdivided into three groups: NPs not linked to the CR sources (separated), NPs bound to the emitters (bound) and NPs incorporating the CR sources (incorporated), often called “self-emitting NPs”. The chemical link must be stable *in vivo* to prevent false localization via imaging techniques, but not all the chemical links are stable or easy to obtain, and thus, the biodistribution of the complex CR source-nanoparticles could be different from that of the NPs. NPs bound and incorporating radioisotopes are a good solution to the problem of excitation distance and colocalization; however, the need to control specific uptake in the target organ remains.

## 2.5. Applications to Cancer Models

Principal biomedical applications are whole body imaging for preclinical investigations, especially for tumor and Lymph nodes detection, endoscopy, and PDT. The most used cell lines for *in vivo* cancer models are 4T1 murine breast cancer [\[21\]\[22\]\[30\]\[35\]\[38\]\[39\]](#) murine mammary carcinoma EMT-6 [\[15\]\[17\]](#), human primary glioblastoma U87 [\[13\]\[16\]\[30\]](#), human fibrosarcoma HT 1080 [\[40\]\[41\]\[42\]](#), and human hepatocellular carcinomas HCC [\[31\]\[32\]](#). The 4T1 murine breast cancer model has been employed mostly for in photodynamic therapy studies [\[21\]\[22\]\[35\]\[39\]](#). It is worth nothing that breast cell lines are very commonly used for testing due to the shallow nature of the associated tumor model, and thus, its *in vivo* detectability, and for the clinical translatability of the results.

## 2.6. CR Sources

Initially, the most widely used CR sources were  $^{18}\text{F}$  and  $^{64}\text{Cu}$  for direct involvement in clinical and preclinical investigations with PET [\[10\]](#), and in particular,  $^{18}\text{F}$  for the widespread use of  $^{18}\text{F}$ -FDG in cancer detection. Subsequently, also  $^{32}\text{P}$  and  $^{68}\text{Ga}$  [\[11\]\[12\]](#) were investigated for their higher production of Cerenkov photons due to their higher endpoint energy, leading to improve *in vivo* detectability. As mentioned, the choice of the radioisotope is important, not only for its

optical emission (related to the activity and to the endpoint energy), but also for its decay mode, which can produce particles which are able to interact with NPs, causing light emission. The principal radioactive sources tested by different authors are  $^3\text{H}$ ,  $^{35}\text{S}$ ,  $^{177}\text{Lu}$ ,  $^{32}\text{P}$ ,  $^{18}\text{F}$ ,  $^{89}\text{Zr}$ ,  $^{68}\text{Ga}$ ,  $^{90}\text{Y}$  and  $^{99\text{m}}\text{Tc}$ , [23].

Considering its therapeutic application in the FDA-approved treatment of patients with gastro-entero-pancreatic neuroendocrine tumors [43], lutetium was investigated as a CR source by Satterlee et al. [25], bound to lipid calcium phosphate NPs—as reported above regarding the lipid nanostructures—as a mode of anticancer therapy in addition to radiographic imaging. Analogously,  $^{188}\text{Re}$ , normally used for bone pain palliation in patients suffering prostate cancer [44], was encapsulated in liposomes by Chang et al. [26] to inhibit proliferation and epithelial-mesenchymal transition of human and neck tumors.

## 2.7. Imaging Techniques

PET imaging is a widely used alternative technique to detect radionuclide-NP complexes. However, SPECT was used by Lee et al. [45], who imaged  $^{125}\text{I}$ -radiolabeled gold nanoparticles. Superparamagnetic iron oxide nanoparticles labeled with  $^{124}\text{I}$  or  $^{18}\text{F}$ -FDG were investigated by [40] to achieve MRI detection of the complex, also in triple optical/PET/MRI modality [39]. It was also reported that the shape-controlled synthesis of rare earth fluoride nanocrystals doped with the  $\beta$ -emitting radioisotope  $^{90}\text{Y}$  may provide a promising platform for multimodal imaging, including MRI [46].

## 3. Photodynamic Therapy Using Cerenkov Sources

The use of light to treat diseases can be dated back to antiquity, as outlined in these two reviews [47][48] focusing on the history of PDT. For example, the ancient Greek physicians, and Herodotus (the father of heliotherapy) in particular, suggested the use of sunlight to treat diseases.

Modern PDT can be traced back to the early 1900s, when the Danish physician, Niels Finsen treated respectively with red or UV light pustules or cutaneous tuberculosis, and was awarded the Nobel Prize in 1903 for his efforts. Around that time, the idea of using light in combination with a drug to kill cells was suggested by Oscar Raab, a medical student who, during a thunderstorm, discovered (by chance) the lethal combination of acridine and light on Infusoria. His supervisor Herman von Tappeiner went on to show the importance of oxygen in the reaction, and in 1907, he introduced the term “photodynamic action”. The basic mechanisms of PDT were thus discovered.

More precisely, PDT is based on the interaction between light at a specific wavelength and a photosensitizer (PS) that is a photo-activatable molecule (at a given wavelength). After the interaction with light, the PS is able to produce reactive oxygen species (ROS), leading to local cytotoxic reactions with cells (Figure 4). Of course, in order to achieve a significant cytotoxic effect, both light and the PS should be available where needed (e.g., inside a tumor region), avoiding normal tissue at the same time. It is thus necessary to develop targeting strategies to enhance the selectivity of the PS and, at the same time, to radiate enough light into the region that needs to be treated. This latter requirement limits the use of PDT, since, due to hemoglobin absorption and tissue scattering, it is not a trivial matter to deliver enough photons to nonsuperficial regions.

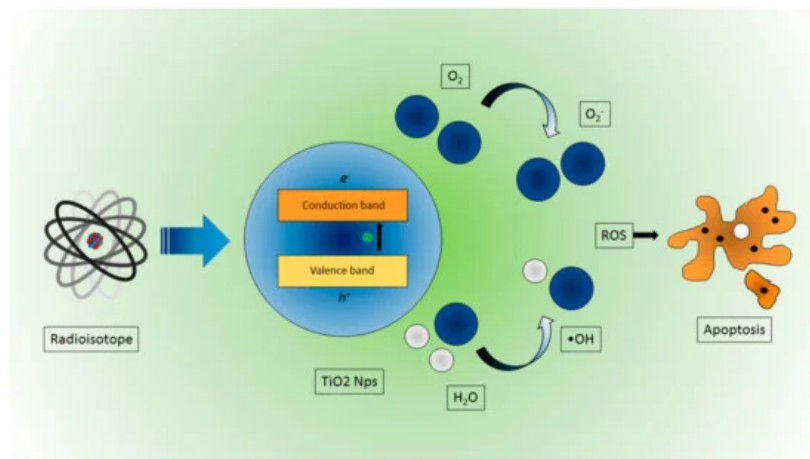


**Figure 4.** Schematic representation of ROS production due to CR interaction in  $\text{TiO}_2$  NPs, leading to cancer cell apoptosis.

In order to solve this problem, there has been, in the recent years, a growing interest in using CR as a local and internal light source, or other external excitation sources like x-rays. The main advantages of using Cerenkov sources are the possibility of bringing the light source as close as possible to the PS and using the UV component of the CR spectrum. This approach was applied by Kotagiri et al. [41]; specifically, transferrin-coated TiO<sub>2</sub> nanoparticles in combination with PET radionuclides like <sup>18</sup>F and <sup>64</sup>Cu were used to perform PDT in vitro and in vivo. They found a strong reduction of cell viability in vitro with respect to control groups when combining radionuclides with the PS. A similar trend was found in vivo using an aggressive HT1080 subcutaneous mouse tumor model. In this case, the tumor volume dropped to almost zero 12 days after treatment, while the controls groups were in the 400–600 mm<sup>3</sup> range. A histological analysis also confirmed extensive tumor necrotic regions.

As mentioned, the number of Cerenkov photons that are produced is dependent on the particle energy. For PDT, it is thus useful to choose, when possible, beta emitter isotopes with higher end point energies in order to obtain a higher yield of Cerenkov photons [49]. Instead of <sup>18</sup>F, Duan et al. [35] suggested the use of <sup>68</sup>Ga (end point energy = 1899 keV), while Hartl et al. [50] proposed the use of <sup>90</sup>Y (end point energy = 2.28 MeV) as an even brighter PDT source with a longer half-life.

Different combinations of radioisotopes and PSs have been investigated, for example in Kamkaew et al. [21], <sup>89</sup>Zr was used as a Cerenkov PDT source to excite chlorin e6 (Ce6), yielding similar in vitro and in vivo results (e.g., lower cell viability and tumor volume) by Kotagiri et al. [41].

In a commentary paper [51], the authors outlined the hypothesis that due to the low yield of Cerenkov emission, an alternative OH radical production mechanism should be sought. It has thus been suggested that an increase in free radical production might be achieved by interactions between direct beta particles and the PS. However, further evidence [51] using ionizing radiation below the Cerenkov threshold showed very little difference in cell viability between groups irradiated with the PS and those without, suggesting the importance of Cerenkov light as a PDT source.

The mechanisms responsible for the creation of electron/hole pairs in the PS need to be further investigated in order to better understand the contribution of possible sources.

---

## References

1. Xu, Y.; Liu, H.; Cheng, Z.; Harnessing the power of radionuclides for optical imaging: Cerenkov luminescence imaging. *J. Nucl. Med.* 2011, 52, 2009–2018.
2. Ma, X.; Wang, J.; Cheng, Z.; Cerenkov radiation: A multi-functional approach for biological sciences. *Front. Phys.* 2014, 2, 1–14.
3. Spinelli, A.E.; Boschi, F.; Novel biomedical applications of Cerenkov radiation and radioluminescence imaging. *Phys. Med.* 2015, 31, 120–129.
4. Tanha, K.; Pashazadeh, A.M.; Pogue, B.W. Review of biomedical Čerenkov luminescence imaging applications. *Biomed. Opt. Express.* 2015, 6, 3053–3065.
5. Shaffer, T.M.; Pratt, E.C.; Grimm, J. Utilizing the power of Cerenkov light with nanotechnology. *Nat. Nanotechnol.* 2017, 12, 106–117.
6. Jacques, S.L. Optical properties of biological tissues: A review. *Phys. Med. Biol.* 2013, 58, R37.
7. Alivisatos, A.P. Semiconductor clusters, nanocrystals, and quantum dots. *Science* 1996, 271, 933–937.
8. Boschi, F.; De Sanctis, F. Overview of the optical properties of fluorescent nanoparticles for optical imaging. *Eur. J. Histochem.* 2017, 61, 2830.
9. Liu, H.; Ren, G.; Miao, Z.; Zhang, X.; Tang, X.; Han, P.; Gambhir, S.S.; Sanjiv, S.; Cheng, Z. Molecular Optical Imaging with Radioactive Probes. *PLoS ONE* 2010, 5, e9470.
10. Dohager, R.S.; Goiffon, R.J.; Jackson, E.; Harpstrite, S.; Piwnica-Worms, D. Cerenkov radiation energy transfer (CRET) imaging: A novel method for optical imaging of PET isotopes in biological systems. *PLoS ONE* 2010, 5, e13300.
11. Boschi, F.; Spinelli, A.E.; Quantum dots excitation using pure beta minus radioisotopes emitting Cerenkov radiation. *RSC Adv.* 2012, 2, 11049–11052.
12. Thorek, D.L.J.; Ogirala, A.; Beattie, B.J.; Grimm, J. Quantitative imaging of disease signatures through radioactive decay signal conversion. *Nat. Med.* 2013, 19, 1345–1350.

13. Sun, X.; Huang, X.; Guo, J.; Zhu, W.; Ding, Y.; Niu, G.; Wang, A.; Kiesewetter, D.O.; Wang, Z.L.; Sun, S.; et al. Self-illuminating  $^{64}\text{Cu}$ -Doped  $\text{CdSe/ZnS}$  nanocrystals for in vivo tumor imaging. *J. Am. Chem. Soc.* 2014, 136, 1706–1709.
14. Zhao, Y.; Shaffer, T.M.; Das, S.; Pérez-Medina, C.; Mulder, W.J.M.; Grimm, J. Near-Infrared Quantum Dot and  $^{89}\text{Zr}$  Dual-Labeled Nanoparticles for in Vivo Cerenkov Imaging. *Bioconjugate Chem.* 2017, 28, 600–608.
15. Wang, Y.; Liu, Y.; Luehmann, H.; Xia, X.; Wan, D.; Cutler, C.; Xia, Y. Radioluminescent gold nanocages with controlled radioactivity for real-time in vivo imaging. *Nano Lett.* 2013, 13, 581–585.
16. Hu, H.; Huang, P.; Weiss, O.J.; Yan, X.; Yue, X.; Zhang, M.G.; Tang, Y.; Nie, L.; Ma, Y.; Niu, G.; et al. PET and NIR optical imaging using self-illuminating  $^{64}\text{Cu}$ -doped chelator-free gold nanoclusters. *Biomaterials* 2014, 35, 9868–9876.
17. Black, K.C.L.; Wang, Y.; Luehmann, H.P.; Cai, X.; Xing, W.; Pang, B.; Zhao, Y.; Cutler, C.S.; Wang, L.V.; Liu, Y.; et al. Radioactive  $^{198}\text{Au}$ -doped nanostructures with different shapes for in vivo analyses of their biodistribution, tumor uptake, and intratumoral distribution. *ACS Nano* 2014, 8, 4385–4394.
18. Volotskova, O.; Sun, C.; Stafford, J.H.; Koh, A.L.; Ma, X.; Cheng, Z.; Cui, B.; Pratx, G.; Xing, L. Efficient Radioisotope Energy Transfer by Gold Nanoclusters for Molecular Imaging. *Small* 2015, 11, 4002–4008.
19. Lee, S.B.; Yoon, G.; Lee, S.W.; Jeong, S.Y.; Ahn, B.C.; Lim, D.K.; Lee, J.; Jeon, Y.H. Combined Positron Emission Tomography and Cerenkov Luminescence Imaging of Sentinel Lymph Nodes Using PEGylated Radionuclide-Embedded Gold Nanoparticles. *Small* 2016, 12, 4894–4901.
20. Lee, S.B.; Li, Y.; Lee, I.K.; Cho, S.J.; Kim, S.K.; Lee, S.W.; Lee, J.; Jeon, Y.H. In vivo detection of sentinel lymph nodes with PEGylated crushed gold shell @ radioactive core nanoballs. *J. Ind. Eng. Chem.* 2019, 70, 196–203.
21. Kamkaew, A.; Cheng, L.; Goel, S.; Valdovinos, H.F.; Barnhart, T.E.; Liu, Z.; Cai, W. Cerenkov Radiation Induced Photodynamic Therapy Using Chlorin e6-Loaded Hollow Mesoporous Silica Nanoparticles. *ACS Appl. Mater. Interfaces* 2016, 8, 26630–26637.
22. Goel, S.; Ferreira, C.A.; Chen, F.; Ellison, P.A.; Siamof, C.M.; Barnhart, T.E.; Cai, W. Activatable Hybrid Nanotheranostics for Tetramodal Imaging and Synergistic Photothermal/Photodynamic Therapy. *Adv. Mater.* 2017, 30, 1704367.
23. Pratt, E.C.; Shaffer, T.M.; Zhang, Q.; Drain, C.M.; Grimm, J. Nanoparticles as multimodal photon transducers of ionizing radiation. *Nat. Nanotechnol.* 2018, 13, 418–426.
24. Genovese, D.; Petrizza, L.; Prodi, L.; Rampazzo, E.; De Sanctis, F.; Spinelli, A.E.; Boschi, F.; Zaccheroni, N. Tandem Dye-Doped Nanoparticles for NIR Imaging via Cerenkov Resonance Energy Transfer. *Front Chem.* 2020, 8, 71.
25. Satterlee, A.B.; Yuan, H.; Huang, L. A radio-theranostic nanoparticle with high specific drug loading for cancer therapy and imaging. *J. Control. Release* 2015, 217, 170–182.
26. Chang, C.Y.; Chen, C.C.; Lin, L.T.; Chang, C.H.; Chen, L.C.; Wang, H.E.; Lee, T.W.; Lee, Y.J. PEGylated liposome-encapsulated rhenium-188 radiopharmaceutical inhibits proliferation and epithelial–mesenchymal transition of human head and neck cancer cells in vivo with repeated therapy. *Cell Death Discov.* 2018, 4, 100.
27. Sun, C.; Pratx, G.; Carpenter, C.M.; Liu, H.; Cheng, Z.; Gambhir, S.S.; Xing, L. Synthesis and Radioluminescence of PEGylated  $\text{Eu}^{3+}$ -doped Nanophosphors as Bioimaging Probes. *Adv. Mater.* 2011, 23, H195–H199.
28. Carpenter, C.M.; Sun, C.; Pratx, G.; Liu, H.; Cheng, Z.; Xing, L. Radioluminescent nanophosphors enable multiplexed small-animal imaging. *Opt. Express* 2012, 20, 11598–11604.
29. Cao, X.; Chen, X.; Kang, F.; Cao, X.; Zhan, Y.; Wang, J.; Wu, K.; Liang, J. Sensitivity improvement of Cerenkov luminescence endoscope with terbium doped  $\text{Gd}_2\text{O}_2\text{S}$  nanoparticles. *Appl. Phys. Lett.* 2015, 106, 213702.
30. Hu, Z.; Qu, Y.; Wang, K.; Zhang, X.; Zha, J.; Song, T.; Bao, C.; Liu, H.; Wang, Z.; Wang, J.; et al. In vivo nanoparticle-mediated radiopharmaceutical-excited fluorescence molecular imaging. *Nat. Commun.* 2015, 6, 7560.
31. Hu, Z.; Zhao, M.; Qu, Y.; Zhang, X.; Zhang, M.; Liu, M.; Guo, H.; Zhang, Z.; Wang, J.; Yang, W.; et al. In Vivo 3-dimensional radiopharmaceutical-excited fluorescence tomography. *J. Nucl. Med.* 2017, 58, 169–174.
32. Hu, Z.; Chi, C.; Liu, M.; Guo, H.; Zhang, Z.; Zeng, C.; Ye, J.; Wang, J.; Tian, J.; Yang, W.; et al. Nanoparticle-mediated radiopharmaceutical-excited fluorescence molecular imaging allows precise image-guided tumor-removal surgery. *Nanomed. Nanotechnol. Biol. Med.* 2017, 13, 1323–1331.
33. Liu, N.; Shi, J.; Wang, Q.; Guo, J.; Hou, Z.; Su, X.; Zhang, H.; Sun, X. In Vivo Repeatedly Activated Persistent Luminescence Nanoparticles by Radiopharmaceuticals for Long-Lasting Tumor Optical Imaging. *Small* 2020, 16, 2001494.
34. Black, K.C.L.; Ibricevic, A.; Gunsten, S.P.; Flores, J.A.; Gustafson, T.P.; Raymond, J.E.; Samarajeewa, S.; Shrestha, R.; Felder, S.E.; Cai, T.; et al. In vivo fate tracking of degradable nanoparticles for lung gene transfer using PET and Cerenkov imaging. *Biomaterials* 2016, 98, 53–63.



35. Duan, D.; Liu, H.; Xu, Y.; Han, Y.; Xu, M.; Zhang, Z.; Liu, Z. Activating TiO<sub>2</sub> Nanoparticles: Gallium-68 Serves as a High-Yield Photon Emitter for Cerenkov-Induced Photodynamic Therapy. *ACS Appl. Mater. Interfaces* 2018, 10, 5278–5286.
36. Lee, S.B.; Kumar, D.; Li, Y.; Lee, I.K.; Cho, S.J.; Kim, S.K.; Lee, S.W.; Jeong, S.Y.; Lee, J.; Jeon, Y.H. PEGylated crushed gold shell-radiolabeled core nanoballs for in vivo tumor imaging with dual positron emission tomography and Cerenkov luminescent imaging. *J. Nanobiotechnol.* 2018, 16, 41.
37. Ferreira, C.A.; Ni, D.; Rosenkrans, Z.T.; Cai, W. Radionuclide-Activated Nanomaterials and Their Biomedical Applications. *Angew. Chem. Int. Ed.* 2019, 58, 13232–13252.
38. Park, J.C.; Yu, M.K.; An, G.I.; Park, S.-I.; Oh, J.; Kim, H.J.; Kim, J.H.; Wang, E.K.; Hong, I.H.; Ha, Y.S.; et al. Facile preparation of a hybrid nanoprobe for triple-modality optical/PET/MR imaging. *Small* 2010, 6, 2863–2868.
39. Ni, D.; Ferreira, C.A.; Barnhart, T.E.; Quach, V.; Yu, B.; Jiang, D.; Wei, W.; Liu, H.; Engle, J.W.; Hu, P.; et al. Magnetic Targeting of Nanotheranostics Enhances Cerenkov Radiation-Induced Photodynamic Therapy. *J. Am. Chem. Soc.* 2018, 140, 14971–14979.
40. Thorek, D.L.; Das, S.; Grimm, J. Molecular imaging using nanoparticle quenchers of Cerenkov luminescence. *Small* 2014, 10, 3729–3734.
41. Kotagiri, N.; Sudlow, G.P.; Akers, W.J.; Achilefu, S. Breaking the depth dependency of phototherapy with Cerenkov radiation and low-radiance-responsive nanophotosensitizers. *Nat. Nanotechnol.* 2015, 10, 370–379.
42. Reed, N.A.; Raliya, R.; Tang, R.; Xu, B.; Mixdorf, M.; Achilefu, S.; Biswas, P. Electrospray Functionalization of Titanium Dioxide Nanoparticles with Transferrin for Cerenkov Radiation Induced Cancer Therapy. *ACS Appl. Bio. Mater.* 2019, 2, 1141–1147.
43. Brown, A. The impact of metastable lutetium 177 on a Nuclear Medicine Department. *J. Nucl. Med.* 2020, 61, 3021.
44. Bieke, L.; de Klerk, J.M. Clinical applications of Re-188-labelled radiopharmaceuticals for radionuclide therapy. *Nucl. Med. Commun.* 2006, 27, 223–229.
45. Lee, S.B.; Ahn, S.B.; Lee, S.W.; Jeong, S.Y.; Ghilsuk, Y.; Ahn, B.C.; Kim, E.M.; Jeong, H.J.; Lee, J.; Lim, D.K.; et al. Radionuclide-embedded gold nanoparticles for enhanced dendritic cell-based cancer immunotherapy, sensitive and quantitative tracking of dendritic cells with PET and Cerenkov luminescence. *NPG Asia Mater.* 2016, 8, e281.
46. Paik, T.; Chacko, A.M.; Mikitsh, J.L.; Friedberg, J.S.; Pryma, D.A.; Murray, C.B. Shape-Controlled Synthesis of Isotopic Yttrium-90-Labeled Rare Earth Fluoride Nanocrystals for Multimodal Imaging. *ACS Nano* 2015, 9, 8718–8728.
47. Daniell, M.D.; Hill, J.S. A history of photodynamic therapy. *ANZ J. Surg.* 1991, 61, 340–348.
48. Ackroyd, R.; Kelty, C.; Brown, N.; Reed, M. The History of Photodetection and Photodynamic Therapy. *Photochem. Photobiol.* 2001, 74, 656–669.
49. Spinelli, A.E.; D'Ambrosio, D.; Calderan, L.; Marengo, M.; Sbarbati, A.; Boschi, F. Cerenkov radiation allows in vivo optical imaging of positron emitting radiotracers. *Phys. Med. Biol.* 2010, 55, 483–495.
50. Hartl, B.A.; Hirschberg, H.; Marcu, L.; Cherry, S.R. Activating Photodynamic Therapy in vitro with Cerenkov Radiation Generated from Yttrium-90. *J. Environ. Pathol. Toxicol. Oncol.* 2016, 35, 185–192.
51. Pratz, G.; Kapp, D.S. Is Cherenkov luminescence bright enough for photodynamic therapy? *Nat. Nanotechnol.* 2018, 13, 354.